Scanning Microscopy

Volume 1992
Number 6 *Signal and Image Processing in Microscopy and Microanalysis*

Article 24

1992

Morphological Filtering and Granulometric Analysis on Scanning Electron Micrographs: Applications in Materials Science

Murielle Prod'homme
Thomson LCC, France

Michel Coster
Université de Caen, France

Liliane Chermant
Université de Caen, France

Jean-Louis Chermant
Université de Caen, France

Scanning Microscopy Supplement 6, 1992 (pages 255-268) 0892-953X/92$5.00+.00
Scanning Microscopy International, Chicago (AMF O'Hare), IL 60666 USA

MORPHOLOGICAL FILTERING AND GRANULOMETRIC ANALYSIS ON SCANNING ELECTRON MICROGRAPHS: APPLICATIONS IN MATERIALS SCIENCE

Murielle Prod'homme[1,2], Michel Coster[2,*], Liliane Chermant[2], Jean-Louis Chermant[2]

[1]Thomson LCC, Av. du Colonel Prat, 21850 St. Apollinaire, FRANCE
[2]Laboratoire d'Etudes et de Recherches sur les Matériaux, LERMAT, URA CNRS n° 1317, ISMRA - Université de Caen, 6 bd. du Maréchal Juin, 14050 Caen Cédex, FRANCE

Abstract

For many applications, scanning electron microscopy (SEM) images reflect the granular texture of analysed objects. So it is important to characterise the morphology of this texture and also to filter these images. Because the size of the texture is the main criterion to be studied, we have focused our paper on granulometric analysis.

We present basic parameters, morphological filtering and granulometry for $\mathbb{R}^n * \mathbb{R}$ functions and their properties with local knowledge and anamorphosis.

Some applications in the domain of materials science illustrate these methods and present their suitable possibilities.

Key Words: Filtering, granulometric analysis, scanning electron microscopy, mathematical morphology, stereology, image analysis, materials science.

*Address for correspondence:
Michel Coster
Laboratoire d'Etudes et de Recherche sur les Matériaux
LERMAT - ISMRA
6 Bd du Maréchal Juin
14050 Caen Cédex, France
Telephone Number: (33) 31 45 26 64
FAX Number: (33) 31 45 26 60

Introduction

In materials science, non planar surfaces are found very often : for example, this is the case of sheet steel surfaces (Jeulin and Jeulin, 1981), fracture surfaces (Coster and Chermant,1983) and ceramic surfaces (Prod'homme *et al.*, 1990).To observe and analyse these surfaces, the scanning electron microscope is the most suitable apparatus because its depth of field is very large at high magnification.

For the scientist, it is very interesting to quantify the information included in these pictures. Image processing and image analysis are very convenient tools for these applications. Different ways are possible to perform image processing and image analysis. Of course, Fourier transform and Fourier analysis can be used to obtain some information on these images. These methods are good to filter the image but it is not easy to interpret the Fourier analysis results (Gauthier, 1991). Mathematical morphology, (Serra, 1982; Serra, 1988; Coster and Chermant, 1989) offers better possibilities especially in the analysis domain.

The scope of this paper is to present a coherent range of morphological methods to filter and analyse the topographic images obtained from scanning electron microscopy (SEM). To illustrate these methods three examples are described : granulometric analysis of carbides in microcrystalline steels, filtering and granulometry on ceramic films and fractographic analysis of microcrystalline steels.

Image Characteristics

Generally, secondary electron images are used in the case of non planar surfaces. In fact, this observation mode gives a perspective image as if the surface was lit by two light sources (Fig. 1). The contrast is mainly topographic but its analysis is very difficult because several phenomena occur : tilt, shading and ridge effects. In practice, this is the reason why it is impossible to reconstruct the true relief without stereopair images.

However, it is true that image texture and surface texture are correlated. In particular, if surface topography is granular, the image texture is also granular.

To analyse non planar surfaces, a reference plane must be defined, (Fig. 2). Generally, it is possible to choose this plane from macroscopical information like the shape of analysed object (metal sheet, ceramic film, ...) or from the knowledge

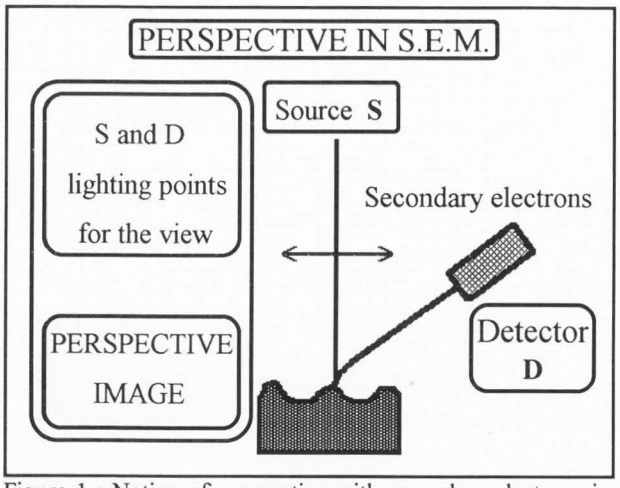

Figure 1 : Notion of perspective with secondary electrons in SEM.

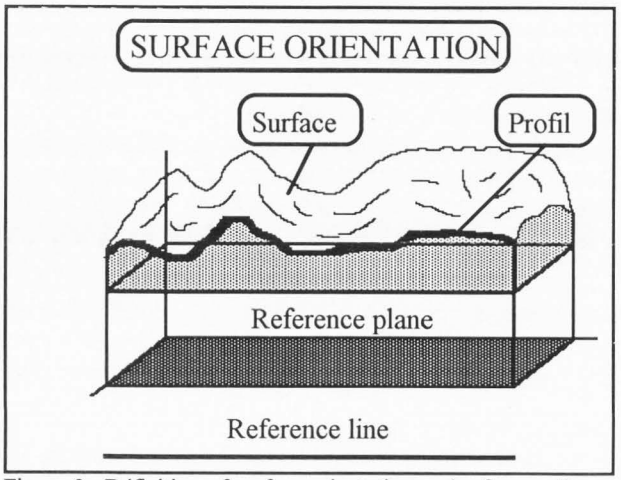

Figure 2 : Définition of surface orientation and reference line.

of main orientation in fracture surfaces. Afterwards, when one presents the morphological methods, the reference plane is assumed to exist and the observation must be perpendicular to this plane.

The topographic images obtained by SEM do not give information on hidden parts (Fig. 3). So one assumes that the analysed surface has no overlapping parts or that the hidden parts are negligible in extent. Under these conditions, it is possible to consider the surface like a relief and the corresponding image as a $\mathbb{R}^2*\mathbb{R}$ function, where $\mathbb{R}^2$ is the support of the function defined in 2D space and $\mathbb{R}$ the radiometric value (grey level value).

Measurements on $\mathbb{R}^2*\mathbb{R}$ Functions

The problem of local knowledge

Generally, the function is known in a bounded mask $Z \in \mathbb{R}^2$. In these conditions, as for set morphology and stereology, the morphological transformations and measures

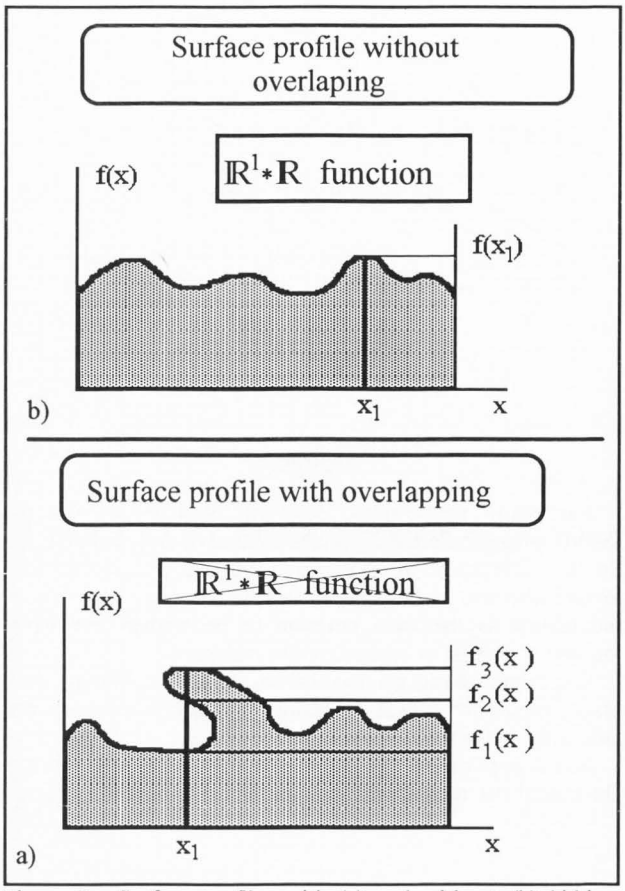

Figure 3 : Surface profiles with (a) and without (b) hidden parts.

on functions must obey to the same laws (Hadwiger conditions), (Hadwiger, 1957).

Hadwiger conditions. For the set analysis in a bounded mask, the measure or image transformation must be :

- invariant with translation (and rotation),
- continuous or, at least, semi-continuous,
- compatible with local knowledge,
- compatible under change of scale.

The third condition is verified if the image transformation is performed by taking the mask of measurement theorem into account (Serra, 1982). The measures having a C-additivity property verify this condition if one uses a correction method (measurements in eroded mask or shell correction method), (Bhanu Prasad *et al.*, 1989).

The three first conditions can be transposed without modifications for the functions $\mathbb{R}^2*\mathbb{R}$. But the fourth condition must be analysed in detail.

Anamorphosis and change of scale. To understand this problem, one compares a function $\mathbb{R}^2*\mathbb{R}$ with a $\mathbb{R}^3$ set. To perform morphological transformation on $\mathbb{R}^3$ set, one uses a 3D structuring element. The sub-graph of the function $\mathbb{R}^2*\mathbb{R}$ can be considered like a set (Fig. 4). Under these conditions, one can also use a 3D structuring element.

Except for true relief analysed like $\mathbb{R}^2*\mathbb{R}$ function, the third dimension ($\mathbb{R}$ value = signal intensity) does not have the

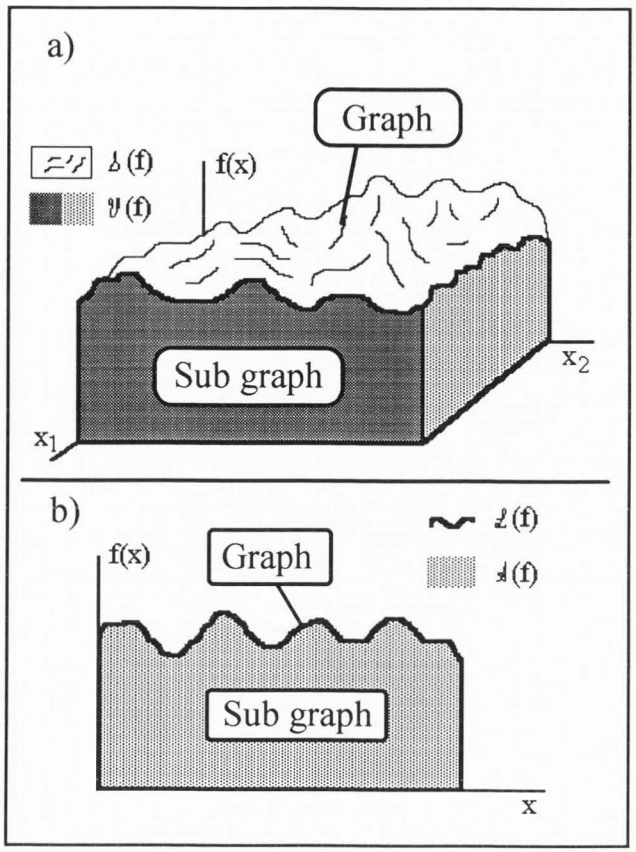

Figure 4 : Définition of graph and sub-graph for $\mathbb{R}^2*\mathbb{R}$ (a) and $\mathbb{R}^1*\mathbb{R}$ (b) functions.

same physical meaning as $\mathbb{R}^n*\mathbb{R}$ dimensions (metric dimensions). The change of scale for the function support ($\mathbb{R}^2$) corresponds to change of magnification, whereas the change of scale for the function value ($\mathbb{R}$) corresponds to a change of signal amplification called *anamorphosis*.

Among the different kinds of anamorphosis, only the cases of *increasing anamorphosis* are considered because in these cases it is possible to have a solution. By definition, an increasing anamorphosis Ψ verifies the following property.

Let f and g be two functions ; Ψ is increasing if :

$$f > g \Rightarrow \Psi(f) > \Psi(g) \qquad (1)$$

Figure 5 presents an example of increasing anamorphosis for $\mathbb{R}^2*\mathbb{R}$ function. Fortunatly most operating condition modifications lead to increasing anamorphosis.

In addition to Hadwiger conditions, the parameters and morphological transformations properties must take into account their behaviour with anamorphosis.

The basic parameters

The basic parameters of $\mathbb{R}^2*\mathbb{R}$ function derive from classical stereological parameters (Minkowsky functionals). These parameters have been defined by Serra (1988) in the case of $\mathbb{R}^2*\mathbb{R}$ functions and have also been discussed by Hénault and Chermant (1992). Let SG(f) be the subgraph and G(f) the graph of the function. Table I presents these parameters and their definition in the global case and Table II in the local case, when the measurement is given in a support of unitary dimension, (Coster,1992).

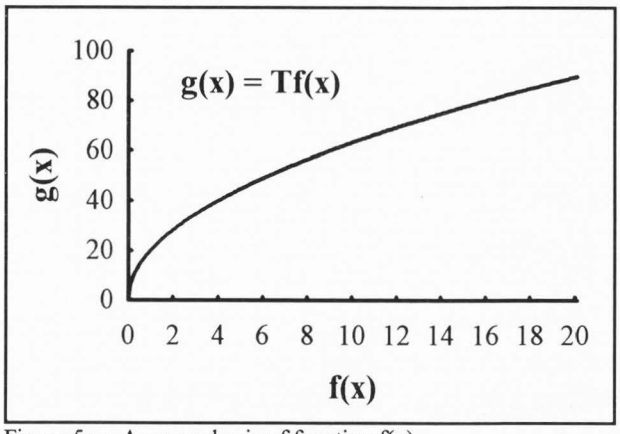

Figure 5a : Anamorphosis of function f(x)

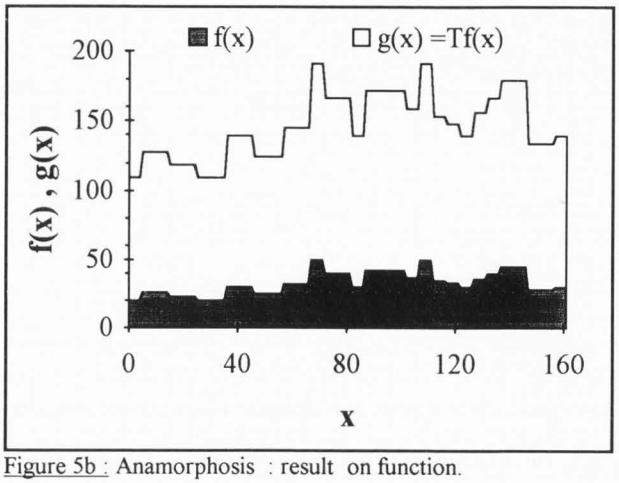

Figure 5b : Anamorphosis : result on function.

In the Table I, Π_t or Δ_t represent respectively the horizontal plane or straight line at the altitude t (the height of the threshold level). The integral of connectivity numbers, $\eta_1(f)$ or $\eta_2(f)$, corresponds to the sum of the local maxima heights minus the sum of local minima heights. The fourth or the third parameter for the set (connectivity number in $\mathbb{R}^3$ or $\mathbb{R}^2$) are not interesting because their values are always 1. These parameters verify Hadwiger properties already described for sets, but they are sensitive to anamorphosis because corresponding definitions have a mixed dimension $\mathbb{R}^n*\mathbb{R}$. As with the set analysis, only some parameters verify Hadwiger's conditions. In the next paragraph, the problem of anamorphosis is treated.

Filtering and Anamorphosis

Filtering methods can be divided into two classes, according to their main properties :

- linear filtering,
- morphological filtering.

Linear filtering

In the case of linear filtering, convolution product and Fourier transforms are used. With these filters, it is impossible to have a transformation which can give a relative result independent of anamorphosis.

Table I : Global parameters for functions.

Function	Measure (global)
	Name and definition (algorithm of measurement)
$\mathbb{R}^2*\mathbb{R}$	volume : $\mathcal{V}(f) = V(SG(f))$ $\left(\mathcal{V}(f) = \int_Z f(x)dx\right)$
$\mathbb{R}^2*\mathbb{R}$	area : $\mathcal{S}(f) = S(G(f))$ (Triangulation, Crofton and Steiner formulae)
$\mathbb{R}^2*\mathbb{R}$	integral of connectivity number $\mathcal{N}_2(f) = \int_{t\in R} N_2(SG(f)\cap\Pi_t)dt$ (Serra method)
$\mathbb{R}^1*\mathbb{R}$	area : $\mathcal{A}(f) = A(SG(f))$ $\left(\mathcal{A}(f) = \int_Z f(x)dx\right)$
$\mathbb{R}^1*\mathbb{R}$	length : $\mathcal{L}(f) = L_2(G(f))$
$\mathbb{R}^1*\mathbb{R}$	integral of connectivity number : $\mathcal{N}_1(f) = \int_{t\in R} N_1(SG(f)\cap\Pi_t)dt$

For example when we modified the image contrast on the SEM, we obtain an anamorphosis. To measure this contrast, the algorithm proposed by Zeboudj (1988) can be used. The contrast **C** for an image of n pixels is defined by:

$$\mathbf{C} = \frac{1}{n}\sum_{i=1y}^{n}\sum_{\in V(x_i)}\left[\frac{C(x_i,y)}{\text{card}V(x_i)}\right] \qquad (2)$$

with $\mathbf{C}(x,y) = |f(x)-f(y)|/(f(x)+f(y))$ defining the contrast between two points, $V(x_i)$ defining the neigbourhood of x_i and $\text{card}V(x_i)$ its cardinal (number of pixels in neigbourhood).

In the case of our apparatus (SEM, JEOL T330), an increasing contrast corresponds to a constant value for the maximum grey level and a decreasing value for the minimum grey level of the image. Under these conditions, an increasing contrast decreases the intensity of the central peak of Fourier spectrum and increases that of other frequencies (Gauthier, 1991) (Fig. 6).

The Fourier spectrum evolution is very complex. This is the reason why, it is impossible to use linear filtering to analyse, in a comparative sense, SEM image textures.

Morphological filtering

The basic morphological image transformations are *erosion* and *dilation*. In the appendix, the erosion and dilation are defined in the case of function. The simplest morphological filters are *opening* and *closing*. The following expression defines the opening for grey tone image by the

Table II : Local parameters for functions.

Function	Measure (local)	Meaning
$\mathbb{R}^2*\mathbb{R}$	$\mathcal{V}_A(f) = \frac{\mathcal{V}(f)}{A(Z)}$	mean value of function
$\mathbb{R}^2*\mathbb{R}$	$\mathcal{S}_A(f) = \frac{\mathcal{S}(f)}{A(Z)}$	equivalent to surface roughness $R_A(G(f))$
$\mathbb{R}^2*\mathbb{R}$	$\mathcal{N}_A(f) = \frac{\mathcal{N}_2(f)}{A(Z)}$	equivalent to vertical roughness for surface : $Rv_A(G(f))$
$\mathbb{R}^1*\mathbb{R}$	$\mathcal{A}_L(f) = \frac{\mathcal{A}(f)}{L(Z)}$	mean value of function
$\mathbb{R}^1*\mathbb{R}$	$\mathcal{L}_L(f) = \frac{\mathcal{L}(f)}{L(Z)}$	equivalent to linear roughness for profile : $R_L(G(f))$
$\mathbb{R}^1*\mathbb{R}$	$\mathcal{N}_L(f) = \frac{\mathcal{N}_1(f)}{L(Z)}$	equivalent to vertical roughness for profile : $Rv_L(G(f))$

structuring function B:

$$O^B f(x) = D^{\check{B}}\left(E^B f(x)\right) \qquad (3)$$

The morphological closing is defined by :

$$F^B f(x) = E^{\check{B}}\left(D^B f(x)\right) \qquad (4)$$

Two kinds of structuring elements can be used (see appendix) :

- volumic structuring element,
- flat structuring element.

In the case of $\mathbb{R}^2*\mathbb{R}$ functions, the volumic structuring element has the same mixed (i.e. non homogeneous) dimensions as the image.

For flat structuring elements, the modulus of the third dimension, corresponding to the radiometric value, is zero. This is the reason why these structuring elements do not change with anamorphosis.

When a morphological filtering is used, the "absolute result" is different between original image and anamorphosed image with any structuring element. But the "relative result" is the same when a flat structuring element is used. So, the ratio between basic measurement performed on the transformed image and an initial image (relative result) is always the same and is independent of anamorphosis. 0f course, this property is not satisfied using a volumic element.

Because opening or closing is an idempotent transformation, to obtain an opening (or closing) of size "n", n erosions (or dilations) followed by n dilations (or erosions) must be performed.

Granulometries on $\mathbb{R}^2*\mathbb{R}$ functions

Granulometric transformation (Serra, 1988) is a class of

Table III : Experimental results on functions of Figures 7a and 7c.

	G(f) according to (5) or (6)	
	Initial (7a)	Initial (7c) = 3*(7a)
opening by (000) flat element	$\frac{52-37}{52}$	$= \frac{156-111}{156}$
closing by (000) flat element	$\frac{56-52}{52}$	$= \frac{168-156}{156}$
opening by (010) flat element	$\frac{52-40}{52}$	$\neq \frac{156-113}{156}$
closing by (000) (flat element	$\frac{58-52}{52}$	$\neq \frac{171-156}{156}$

basic morphological filtering (opening or closing) when the structuring element is convex and depends on size criterion λ. The variation of λ gives a family of similar structuring elements.

The granulometries are very well adapted tools for $\mathbb{R}^2*\mathbb{R}$ functions. Moreover they were the first morphological tools used to analyse grey tone images (Michelland *et al.*, 1989). Matheron's axioms can be used for functions $\mathbb{R}^n*\mathbb{R}$ (Matheron, 1975; Serra, 1988; Coster and Chermant, 1989). It is therefore possible to obtain granulometric distribution in measure.

The granulometric distribution is then given by :

$$G(f_{\lambda B}) = \frac{mes(f) - mes\left(O^{\lambda B} f\right)}{mes(f)} \qquad (5)$$

where $O^{\lambda B} f$ is a morphological opening of the function by the convex structuring function B of size λ and "mes" the basic parameter $\mathcal{V}$ for $\mathbb{R}^2*\mathbb{R}$ and $\mathcal{A}$ for $\mathbb{R}^1*\mathbb{R}$.

With closings $F^{\lambda B} f$, one obtains an antigranulometric distribution, given by :

$$G\left(f^{\lambda B}\right) = \frac{mes\left(F^{\lambda B} f\right) - mes(f)}{mes(f)} \qquad (6)$$

The granulometric density (size density), $g(f_{\lambda B})$ or $g\left(f^{\lambda B}\right)$, is obtained by derivation of $G(f_{\lambda B})$ or $G\left(f^{\lambda B}\right)$.

When the structuring element is flat, the granulometric distribution is independent of increasing anamorphosis. This property is illustrated in Figures 7a and 7b. This is a very important property for applications. It implies, for example, that the result is independent of signal amplification before acquisition of the image or during analog-digital conversion

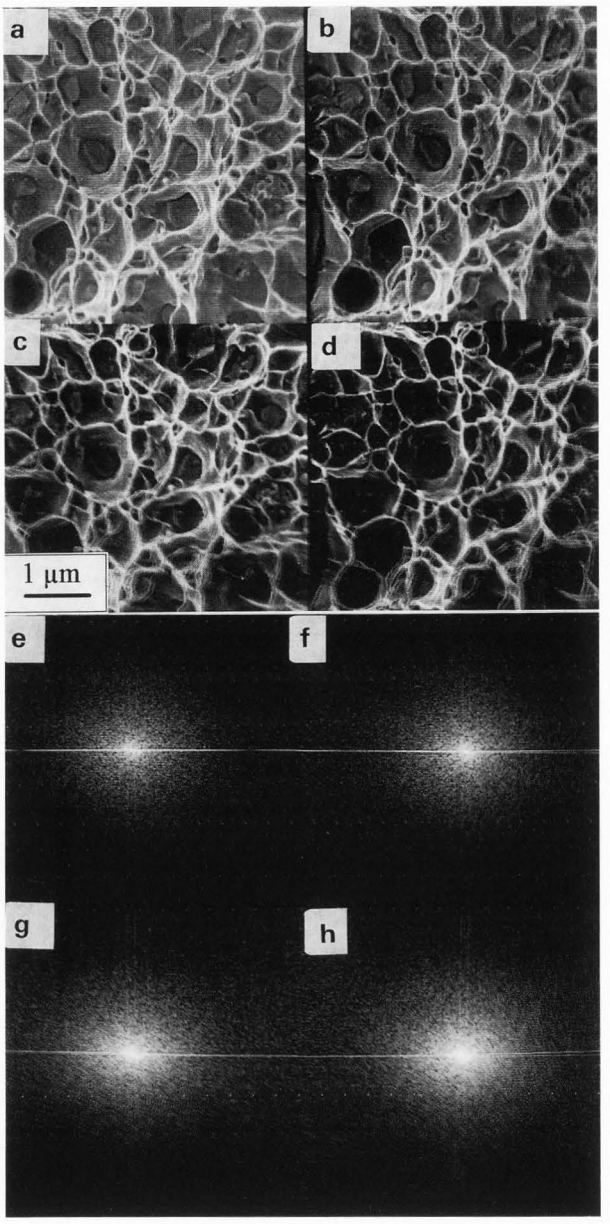

Figure 6 : Contrast increasing from a to d and Fourier spectrum (e-h), (the image is normalised according to the central peak).

(Table III).

Figures 7c and 7d illustrate the opening and closing with non flat structuring element. In this case the result depends on anamorphosis (Table III).

For comparison Figure 8 shows a linear filtering obtained by convolution product on the same function as Figure 7. In this case, the volume of the filtered image is always the same as the volume of initial image, if the coefficients of neighbourhood function are positive ($G(\lambda) = 0$). So, it is impossible to perform granulometric analysis by linear filtering.

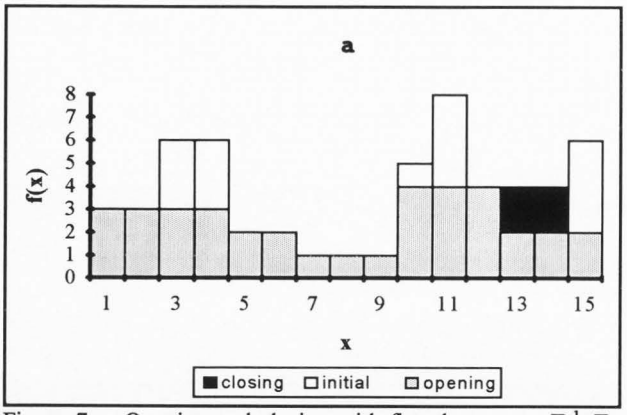

Figure 7a : Opening and closing with flat element on $\mathbb{R}^1 * \mathbb{R}$ function.

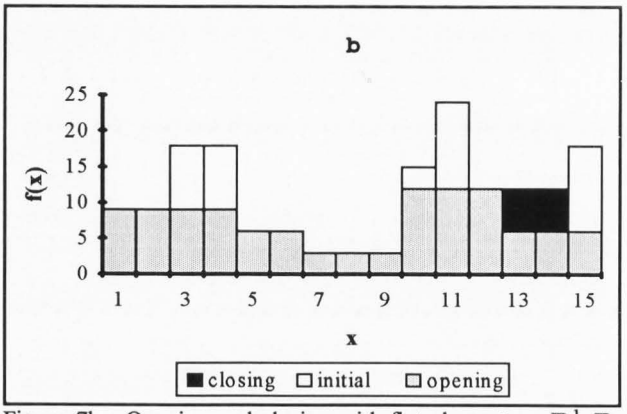

Figure 7b : Opening and closing with flat element on $\mathbb{R}^1 * \mathbb{R}$ function of figure 7a multiplied by 3.

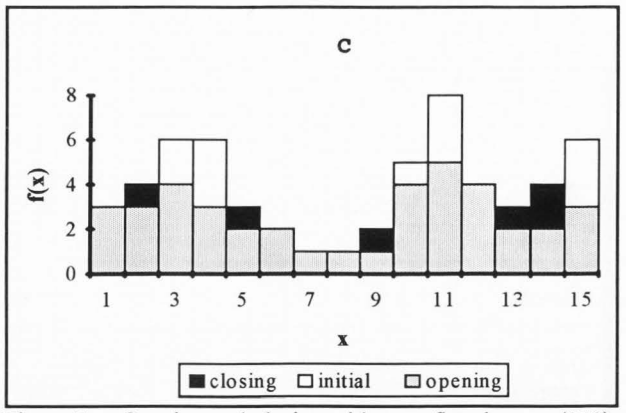

Figure 7c : Opening and closing with non-flat element (010) on $\mathbb{R}^1 * \mathbb{R}$ function of figure 7a.

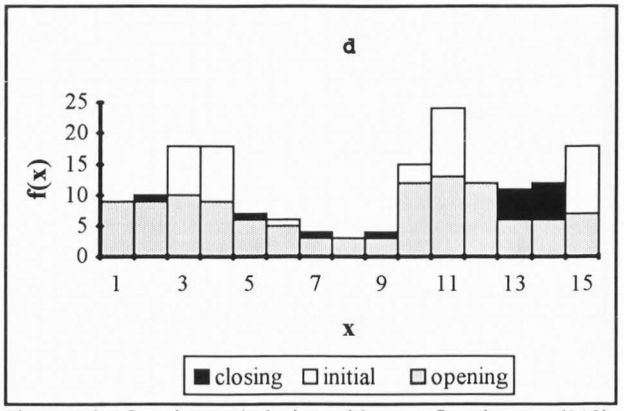

Figure 7d : Opening and closing with non-flat element (010) on $\mathbb{R}^1 * \mathbb{R}$ function of figure 7a multiplied by 3.

Examples of Applications

To perform such an analysis, a system composed of a SUN 3/140 computer coupled with an image processor IMAGING TECHNOLOGIES series 151 in a VISILOG software environment was used. The transformations have been performed with a square grid.

Granulometric analysis of carbide particles

Steels with high carbon content, obtained by extrusion of microcrystalline powders, contain a high ratio of carbides. Due to their small size, they can be observed only by SEM. To reveal their granular texture, such specimens must be deeply etched to create a granular relief. A granulometry by opening on grey tone images provide indirect access to the carbide grain size distribution.

Figure 9 illustrates the image transformation for different opening sizes. To obtain the granulometric distribution according to the formula (5), the volume of the function was measured after each opening. Of course the result depends on the shape of the structuring function, (here cubic umbrae or square cylinder) : this is the same problem as with sieving. It is possible to use structuring functions more "circular", but the computerization is more difficult. In a previous paper Michelland *et al.*, 1989), it has been shown that the granulometric distribution changes only a little when an hexagonal prismatic umbrae or hexagonal cylinder were used.

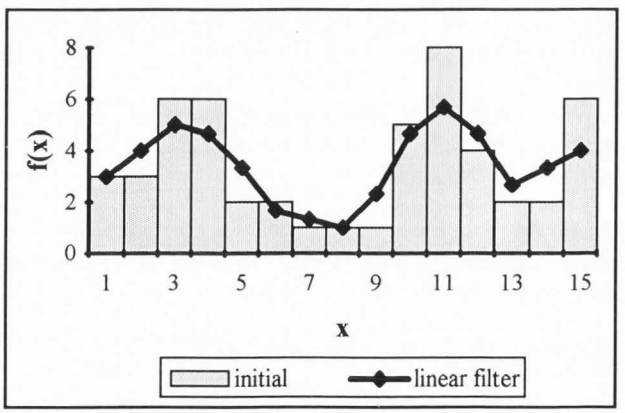

Figure 8 : Linear filtering (convolution product by (111) on function of figure 7a.

As a first step, we verified that variations in the conditions of data acquisition had no influence on the results of the granulometric analysis.

This experiment has been realised from SEM micrographs via CCD camera. From Figure 10, we note that an anamorphosis produced by a change in the (aperture) diaphragm value and in the camera gain does not change the size distribution. It is the same when astigmatism and focus values are

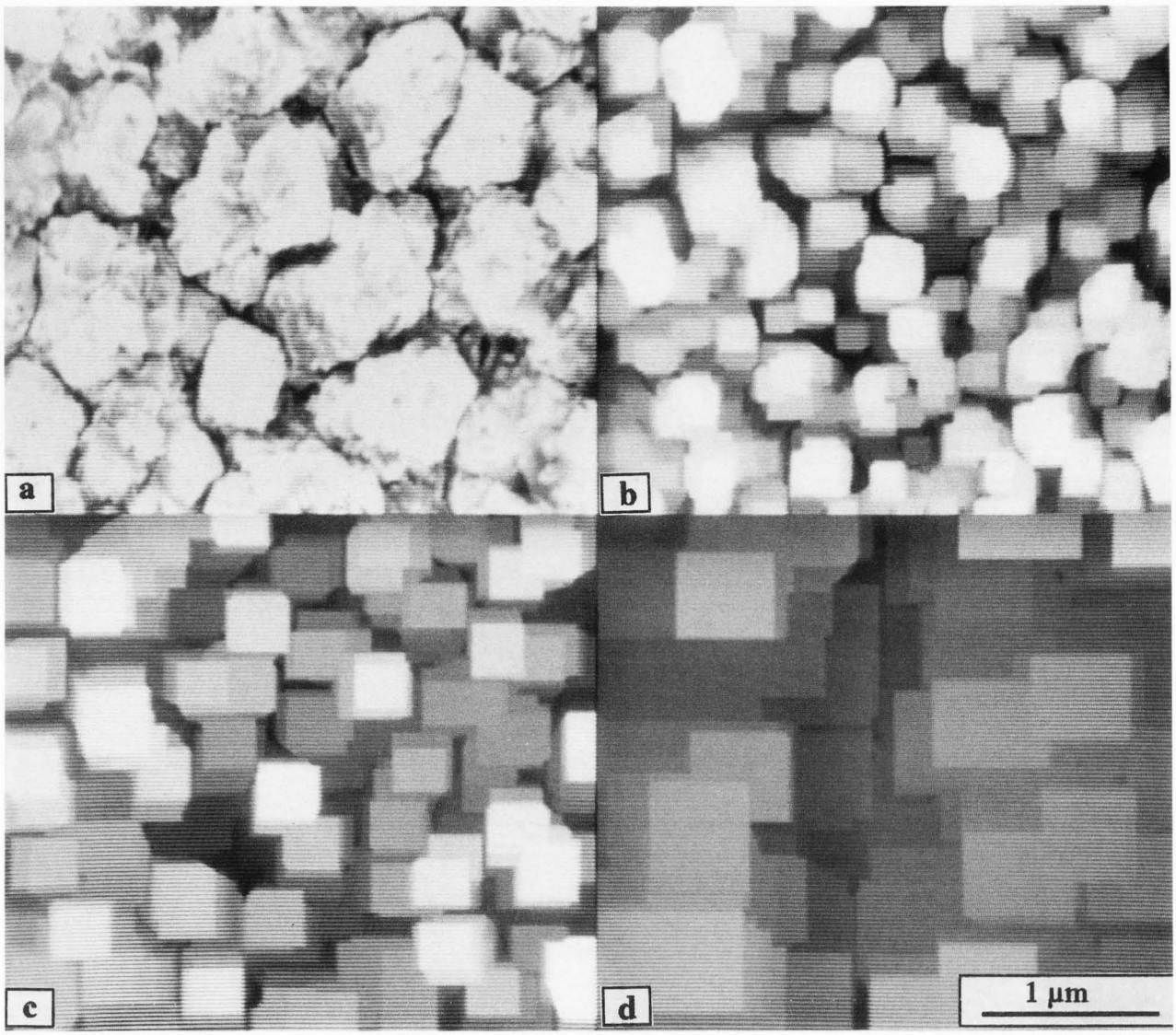

Figure 9 : Morphololological opening of increasing size on image of microcrystalline steels deeply etched by nital and obseved with SEM in secondary electron mode.
Figure 9a : initial image. Figure 9b : opening of size 5 pixels with flat cubic structuring element. Figure 9c : opening of size 10 pixels with flat cubic structuring element. Figure 9d : opening of size 15 pixels with flat cubic structuring element.

changed on the SEM, (Fig. 11).

As explained above, the basic hypothesis at the root of this investigation was that the texture was induced by the granular nature of carbide crystals. To verify this hypothesis, a comparison with a semi-automatic analysis using a digitizing tablet was performed.

With the cursor of the tablet, the outline of each carbide crystal was drawn and the corresponding surface area was measured. Figure 12 presents the results obtained in that way: it is in remarkable agreement with that given by the opening method.

So, it has been found possible to follow the change in the carbide size in microcrystalline steels as a function of the atomisation conditions of the initial powder, of the carbon content and of the thermal treatment (Michelland, 1990). It was shown that the carbide size decreased with thermal treatment.

Texture analysis of ceramic films

The morphological characteristics of dielectric ceramic sheets obtained from tape casting during the manufacture of electronic components depend on the process route conditions.

Scanning electron images (Fig. 13) of green tapes have been analysed (Prod'homme *et al.*,1990). The granular texture of these sheets can be characterised by grey tone level granulometry. The transformation used here involved opening by a flat structuring element of size l, because the segmentation of the image to obtain isolated grains is not

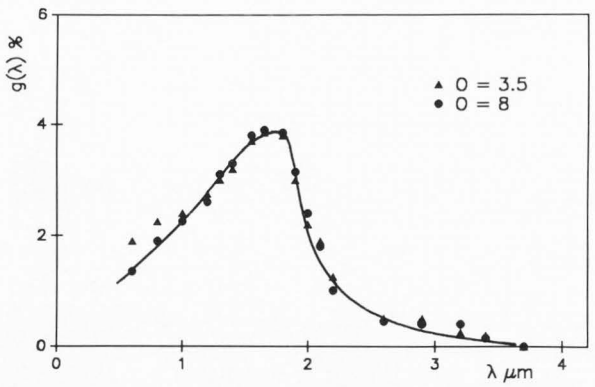

Figure 10 : Granulometric density g(λ) for an area of the same microcrystalline steel photographed with different aperture values.

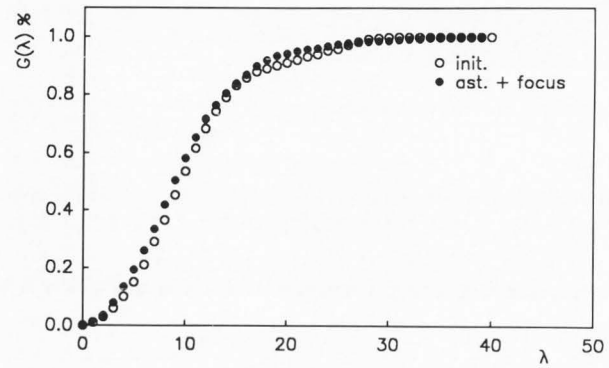

Figure 11 : Granulometric distribution G(λ) for an area of the same microcrystalline steel photographed with different values of astigmatism and focus.

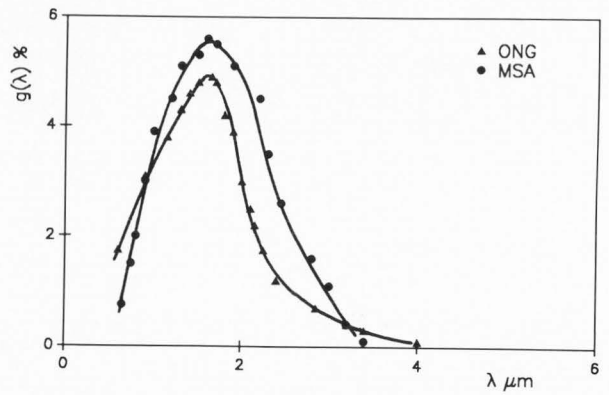

Figure 12 : Results on the size distribution by semi-automatic method (MSA) and by grey tone level opening method (ONG) on the same microcrystalline steel.

possible, (see histogram of grey tone levels, (Fig. 14)).

On these materials, another morphological analysis has been performed using automatic thresholding to separate pores from grains (Prod'homme *et al.*, 1992). Before performing this thresholding, we have used an automedian filter (Serra, 1988) made of a flat square element of four pixels which is not sensible to anamorphosis.

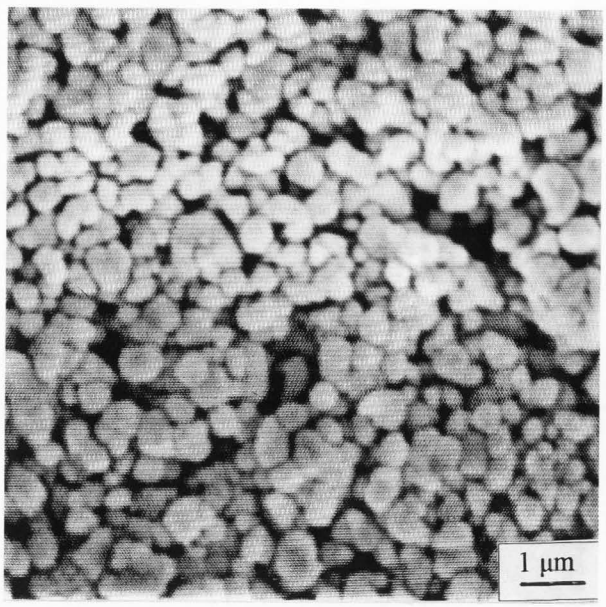

Figure 13 : Grey tone level image of ceramic green tape ($BaTiO_3$) (SEM image).

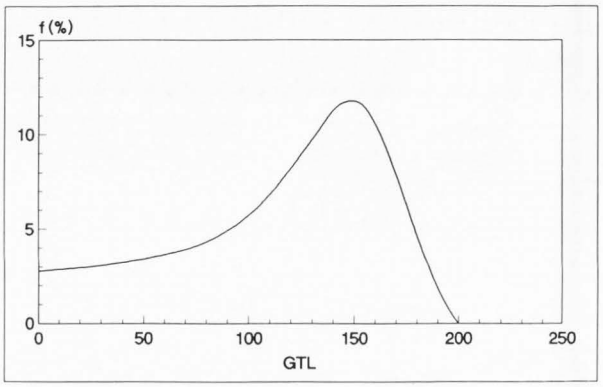

Figure 14 : Histogram of grey tone levels (GTL) of the image of figure 13.

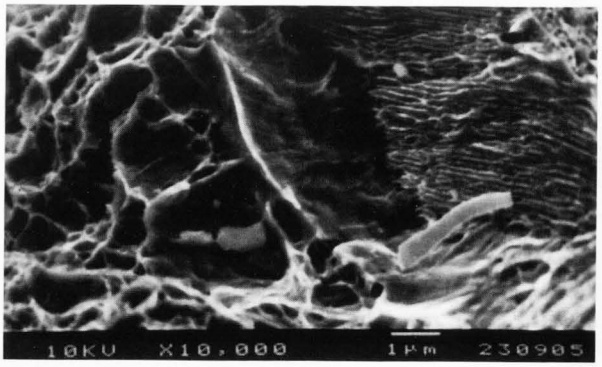

Figure 15 : Scanning electron fractograph of microcrystalline steel fractured in three-point bending.

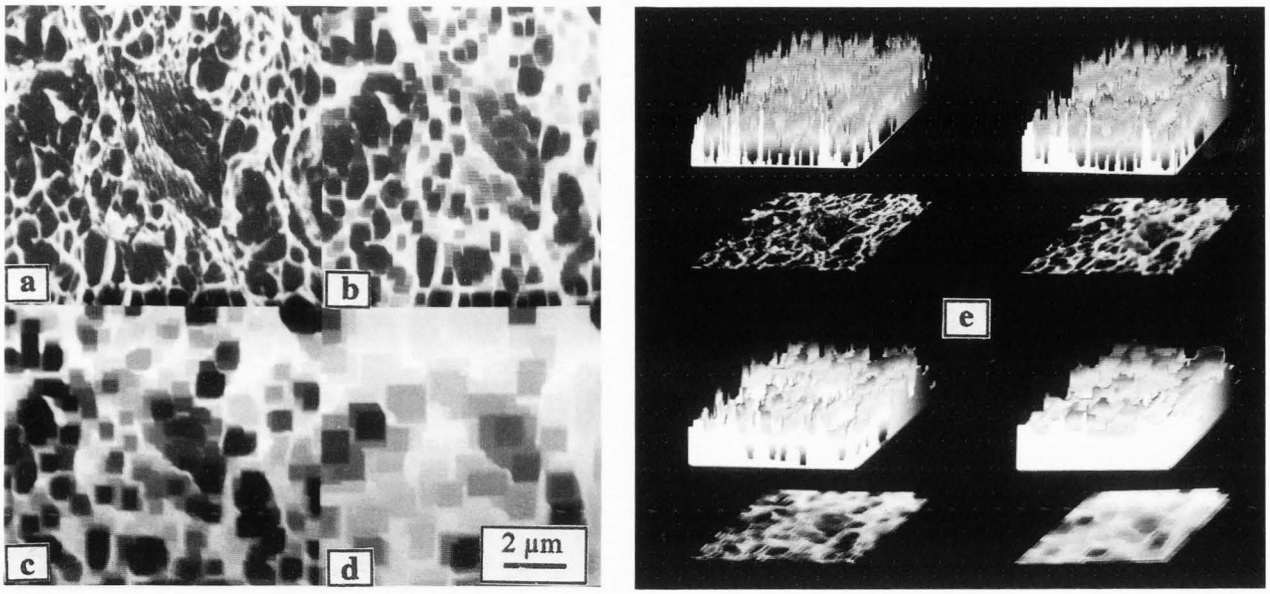

Figure 16 : Effect of closing on a fractograph.
Figure 16a : initial image. Figure 16b : same image after closing of 3 pixels by a flat cubic structuring element. Figure 16c : same image after closing of 5 pixels by a flat cubic structuring element. Figure 16d : same image after closing of 10 pixels by a flat cubic structuring element. Figure 16e : corresponding image of figures 16a to d in pseudo 3D perspective.

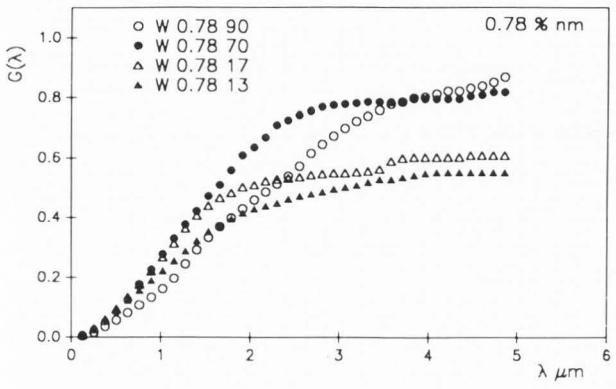

Figure 17 : Granulometric size distribution G(λ), for different microcrystalline steels (O.78% C, powder diameter : 13, 17, 70 and 90 µm).

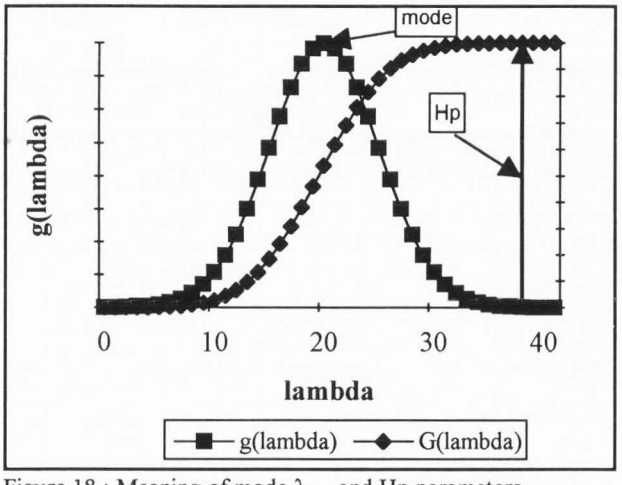

Figure 18 : Meaning of mode λ_m, and Hp parameters.

It was thus possible to quantify the evolution of the texture size with the time of ball milling and the nature of the shape of the balls (spheres or cylinders). An increasing time of ball milling gives finer textures and the effect is more pronounced when milling with cylinders.

Quantitative fractography of microcrystalline steels

Fracture surfaces of several microcrystalline steels were also analysed using SEM, (Fig. 15), (Michelland, 1991). Our attention focused on two morphological characteristics: the percentage of ductile zones and the size of the dimples.

To separate these two feature types, the image must be filtered. We notice that the "size" of the texture in the ductile zones is smaller than the size of the texture in the brittle zones. The most appropriate filter is a closing using a flat structuring element because this transformation mainly modifies the ductile zones and because the closing has adequate properties to perform granulometric analysis.

Figure 16 illustrates this transformation. Some size distribution curves are presented in Figure 17. Two parameters can be derived from these curves:

- the first mode of the distribution which corresponds mathematically to the first inflexion point on the distribution curve (Fig. 18) and physically to the "mean" size of the dimples,
- the height of the plateau which can be correlated to the percentage of dimples, because for this closing size all dimples are removed.

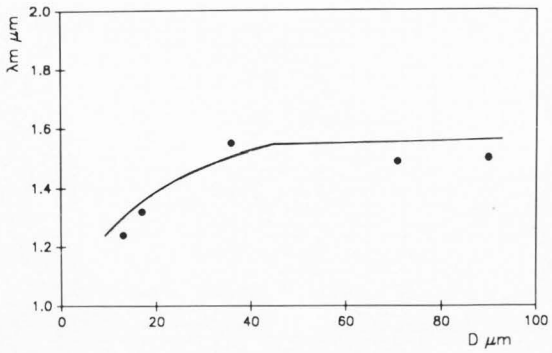

Figure 19 : Change in the dimple size λ_m,with the size of initial powder.

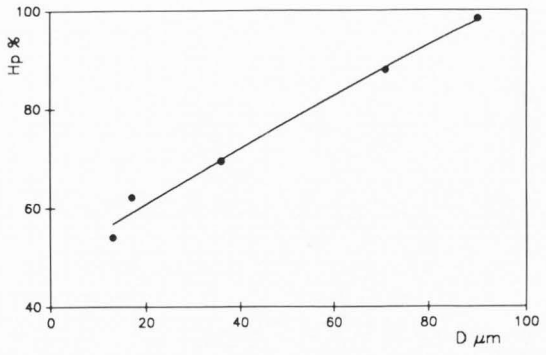

Figure 20 : Change in the plateau height Hp, as a function of powder size, D.

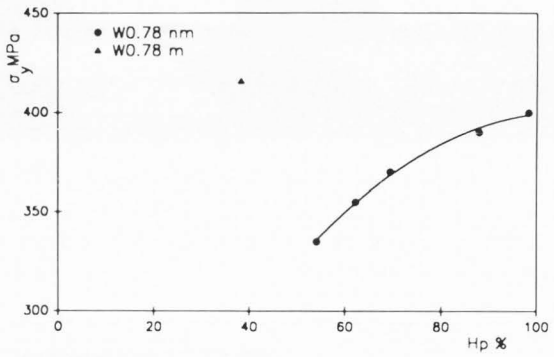

Figure 21 : Change in the yield stress σ_y, as a function of the plateau height.

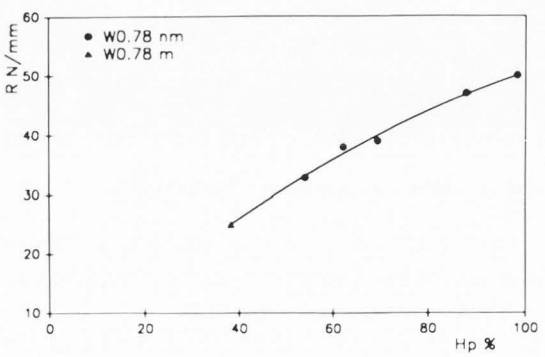

Figure 22 : Change in the crack growth resistance, as a function of the plateau height.

These parameters are correlated to the size of the initial steel powder used before extrusion process (Fig. 19 and 20). The height of the plateau is also correlated to the mechanical properties, as yield stress (Fig. 21) or crack growth resistance (Fig. 22).

Conclusions

In this paper, a set of powerful and coherent methods was presented to analyse quantitatively grey tone images obtained from SEM. These methods use mainly mathematical morphology principles and morphological filters. We have also described the basic parameters useful for these analyses. The problem of the local knowledge and the problem of anamorphosis have been treated. Some examples of texture analysis, choosing in the domain of materials science, illustrate these methods. It can be noted that we have used only the volume to quantify our analysis, but other parameters can be also used in the same manner.

Appendix:

Mathematical Morphology for Functions

Erosion and dilation in set morphology

To define the operation of erosion, let us picture ourselves in $\mathbb{R}^2$ space partially occupied by a set X. Let us now take a structuring element B_X of simple geometrical shape, and, labelling it by its centre, place it at a position x in the space $\mathbb{R}^2$ (Fig. A1): then let us subsequently displace it so that it occupies successively all other positions x in the space. At each place we enquire : is B_X completely included in X: $B_X \subset X$? The positions x for which the answer is "yes" belong to a new set Y said to be the erosion of X by B. This set satisfies the equation :

$$Y = E^B(X) = \{x : B_x \subset X\} \qquad (A1)$$

When the structuring element is a more and less isotropic convex set (square, hexagon,...), the erosion removes one or more layers of pixels from the boundaries of the set (Fig. A2). That is not the case with a concave structuring element.

The operation of dilation is defined in a similar way. Using the same structuring element B we enquire, for each position in $\mathbb{R}^2$: does B_X touch X, $(B_X \hat{\Uparrow} X)$? The set of positions for which the answer is "yes" belongs to a new set Y :

$$Y = D^B(X) = \{x : B_x \hat{\Uparrow} X\} = \{x : B_x \cap X \neq \varnothing\} \quad (A2)$$

In the case of convex structuring elements, the dilation adds layers of pixels around the boundaries of the set (Fig. A3).

The dilation and erosion having an iterative property, it is possible to perform an erosion or dilation of size n with n erosions or dilations of size 1 (this is not true for opening and closing).

Erosion and dilation of functions

The use of umbrae is the better way to go from set morphology to mathematical morphology for function. The umbrae of the function is the set of points (x,t) below the

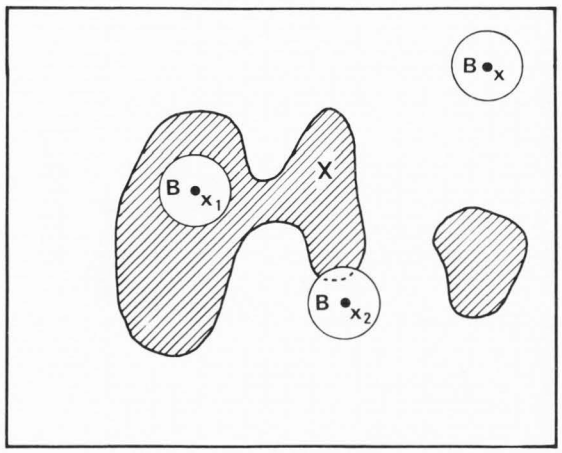

Figure A1 : Hit or miss transformation with a structuring element B_X.

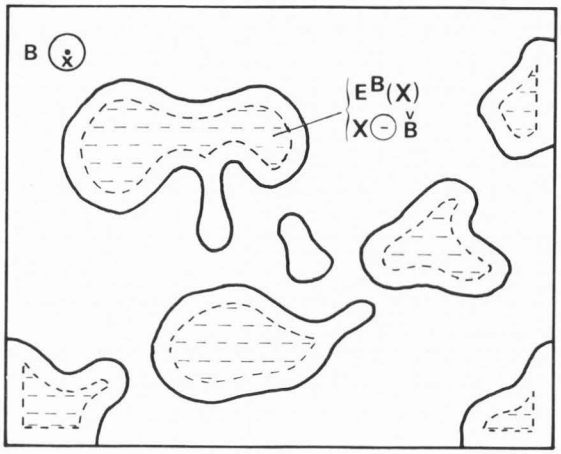

Figure A2 : Set and eroded set.

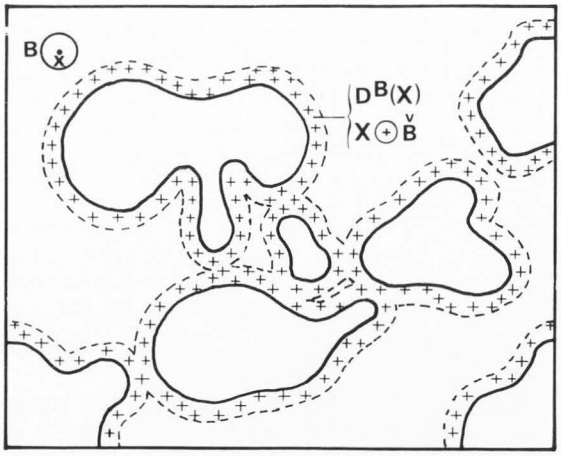

Figure A3 : Set and dilated set.

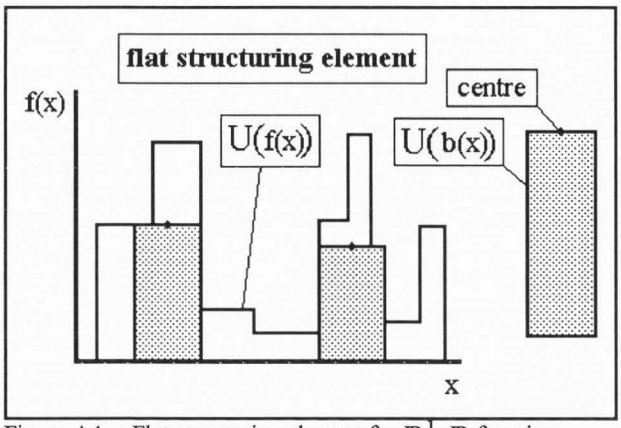

Figure A4a : Flat structuring element for $\mathbb{R}^1 * \mathbb{R}$ function.

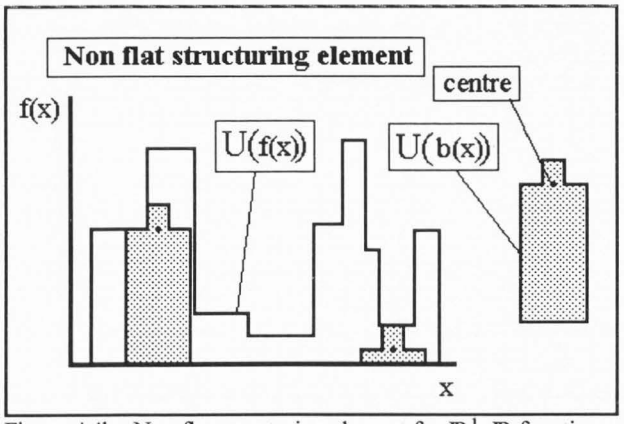

Figure A4b : Non flat structuring element for $\mathbb{R}^1 * \mathbb{R}$ function.

graph:

$$U_f = \left\{ \underset{x \in R^n}{x,t} \; : t \le f(x) \right\} \qquad (A3)$$

Let be a function $\mathbb{R}^1 * \mathbb{R}$ and its sub-graph and let b(u) be a structuring function defined on the support B' and its umbrae B (Fig. A4). The erosion of U_f by B is then given by :

$$E^B(U_f) = \left\{ x,t : B_{x,t} \subset U_f \right\} \qquad (A4)$$

When b(u) is always equal to zero, one defines a flat structuring function (element).

To dilate a function by a plane structuring element, we need to attribute to point x the upper value f(x) in the domain B'_x . So we may write :

$$D^B(f(x)) = \sup\left\{ f(u) : u \in B'_x \right\} \qquad (A5)$$

Similarly, to erode the function the lower value of f(x) must be taken :

$$E^B(f(x)) = \inf\left\{ f(u) : u \in B'_x \right\} \qquad (A6)$$

Although it is not often, this generalisation can be extended by considering structuring elements defined in $\mathbb{R}^2 * \mathbb{R}$ instead of flat ones. A non-flat structuring element B_X can be constructed from the plane structuring element B'_x (projection of B_X on OZ) by associating with the point u belonging to B'_x the height of the boundary of B_X in u. For each point u belonging to B'_x, a function b(u) is thus defined.

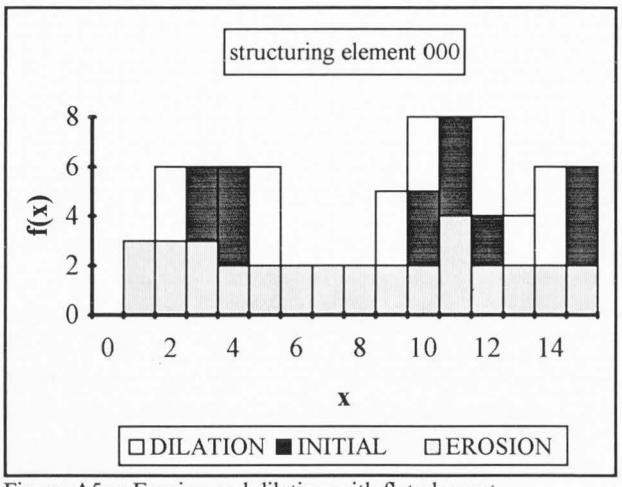

Figure A5a : Erosion and dilation with flat element.

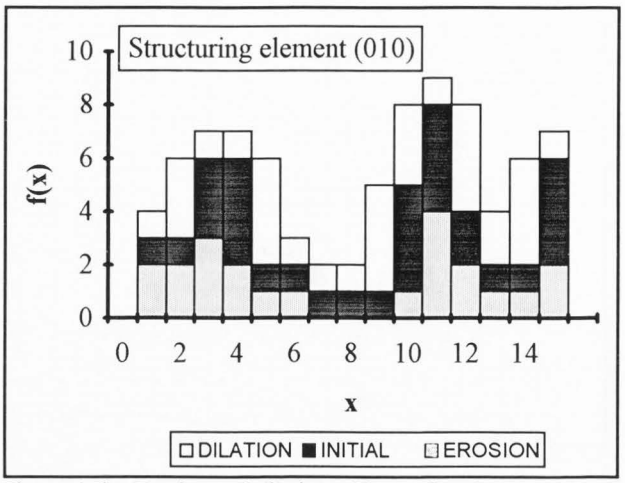

Figure A5b : Erosion and dilation with non flat element.

Dilation is then expressed by :

$$D^B(f(x)) = \sup\{f(u) + b(u) : u \in B'_x\} \quad (A7)$$

and erosion by :

$$E^B(f(x)) = \inf\{f(u) - b(u) : u \in B'_x\} \quad (A8)$$

The difference between a flat and a non-flat structuring element is easily shown for an image defined in $\mathbb{R}^1$ (Fig. A5). Erosion and dilation by a flat structuring element in $\mathbb{R}^1$ (straight line segment) gives rise to Figure A5a, while, if the same Figure is eroded by a non-flat structuring element in $\mathbb{R}^1$, Figure A5b is obtained.

Functions associated with certain convex polyhedra are easily determined for an hexagonal or a square grid. The Figures A6 to A8 illustrate the umbrae obtained with main flat and volumic structuring elements.

These elements have the size "1". To obtain an erosion or dilation of size "n", one can use the classical following algorithm :

```
'initial image in matrix M1
'working image M2
DECLARE ERODE (source,destination,element)
DECLARE COPY (source, destination)
DECLARE DILATE (source destination,element)

OPENING OF SIZE N :
    I = 0
    DO UNTIL I = N
        ERODE (M1,M2,B)
        COPY (M2,M1)
        I = I + 1
    LOOP
    I = 0
    DO UNTIL I = N
        DILATE (M1,M2,B)
        COPY (M2,M1)
        I = I + 1
    LOOP
```

Acknowledgements

We want to particularly thank Dr. Sophie Michelland-Abbé for the presentation of examples related to microcrystalline steels.

References

Bhanu Prasad P, Lantuejoul C, Jernot JP, Chermant JL (1989) Unbiased estimation of the Euler-Poincaré characteristic. Acta Stereol **8**, 101-106.

Coster M, Chermant JL (1983) Recent developments in quantitative fractography. Intern Met Rev **28**, 228-250.

Coster M, Chermant JL (1989) Précis d'analyse d'images (Handbook of image analysis). Ed. Les Presses du CNRS, Paris, France.

Coster M (1992) Morphological tools for non planar surfaces. Acta Stereol, **11/S1**, 639-650.

Gauthier G (1991) Influence des conditions d'acquisition sur la texture des images MEB en électrons secondaires, modélisation de structures aléatoires 3D (Influence of image acquisition conditions on the texture of secondary electron SEM images, modelling of random 3D structures). Mémoire de DEA "Instrumentation et Commande", Université de Caen, France (copy available from M. Coster).

Hadwiger H (1957) Vorslesungen über Inhalt, Oberfläche und Isoperimetrie (Lectures on Shape, Surface and Isoperimetry). Springer-Verlag, Berlin, Germany.

Henault E, Chermant JL (1992) Parametrical investigation of grey tone image. Acta Stereol **11/S1**, 665 - 670.

Jeulin D, Jeulin P (1981) Synthesis of rough surfaces by random morphological models. Stereol Iugosl **3/1**, 239 - 246.

Matheron G (1975) Random sets and integral geometry. J. Wiley, New York, USA.

Michelland S, Schibborr B, Coster M, Mordike BL, Chermant JL (1989) Size distribution of granular materials from unthreshold images. J. Microscopy **156**, 303-311.

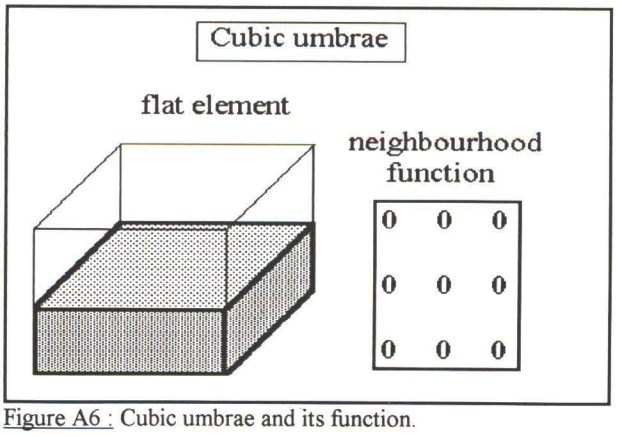

Figure A6 : Cubic umbrae and its function.

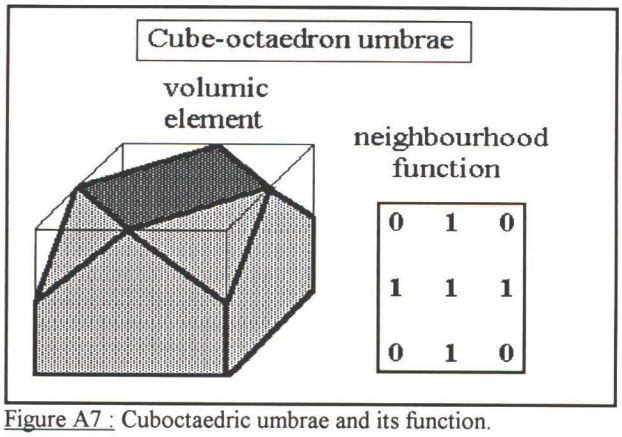

Figure A7 : Cuboctaedric umbrae and its function.

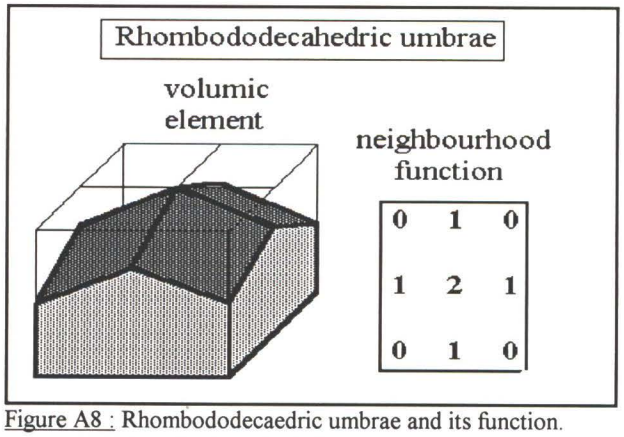

Figure A8 : Rhombododecaedric umbrae and its function.

Michelland-Abbé S (1990) Morphologie et comportement mécanique d'aciers microcristallins extrudés (Morphology and mechanical behavior of extruded microcristalline steels). Thesis, Université de Caen, France.

Michelland-Abbé S, Coster M, Chermant JL, Mordike BL (1991) Quantitative fractography of microcristalline steels by automatic image analysis. J. Comp Ass Micros **3**, 23-32.

Prod'homme M, Chermant L, Coster M, Chermant JL (1990) Etude de la texture de films céramiques par analyse d'images (Study of the texture of ceramic films by image analysis). Troisième Journées Nationales d'Etudes: "Technologie des céramiques pour l'électronique et l'électrotechnique", CNET-SEE, Lannion, France, 15-16 Mai, Paper 0-8 (copy available from M. Coster).

Prod'homme M, Chermant L, Coster (1992) M Texture analysis of ceramic films by image processing. Acta Stereol **11/S1**, 261-266.

Serra J (1982) Image analysis and mathematical morphology. Academic Press, London, UK.

Serra J (1988) Image analysis and mathematical morphology : vol. II theoretical advances. Academic Press, London, UK.

Zeboudj R (1988) Du pré-traitement à l'analyse d'image (From image preprocessing to image analysis). Doctorate Thesis, Université de Saint Etienne, France.

Discussion with Reviewers

N. K. Tovey : Your approach seems to be of great utility in many disciplines, some of which use words which are similar to those use you use, but have different meaning. Could you please briefly explain, for those not familiar with steels, what the dimples are? I presume these are real features and not descriptions of features on the images after processing? Also the reference to the word "plateau", does this refer to the asymptotic value in Figure 19 - i.e. the quantity H_P?

Author : Yes indeed, the dimples are real features which occur on fracture surface of materials when they are fractured after a plastic deformation. During the plastic flow some cavities appear to triple boundaries or to precipitates. On the fracture surfaces these cavities are called dimples. This a typical feature of ductile material. In image processing it is possible to separate, by closing, ducile zones from brittle zones because the texture of dimple zone has not the same size that the texture of brittle zone.

When we perform granulometric analysis by closing, we obtain curves like Figure 17. From these curves we define two parameters λ_m and H_P (Figure 18). The asymptotic value of Figure 19 does not correspond to the plateau height but shows that the size of dimple become independent of the size of the powder for the larger one. Whereas H_P is always function of the size of the powder (Figure 20). The plateau height correspond approximately to the proportion of ductile zones on fracture surface. This the reason why H_p is correlated to mechanical properties (Figures 21 and 22).

N. K. Tovey : You indicate, that to check your results, you used a semi-automatic method using a digitizing tablet with which you defined the outlines of each crystal. I cannot see how this is semi automatic, as presumeably it is entirely dependant on the operator to define the outline?

Author : In the world of image analysis, semi-automatic methods use digitizing tablet to input the data from images. In this case the operator draws the outline and the computer transforms the input coordinates in term of morphological parameters by an automatic routine.

P. Smart : This is an important paper showing the usefulness of some new methods of image analysis and many engineers and scientists will wish to adapt their own instruments to perform similar analyses. I would be very helpful if the authors would clarify the meaning of size of an opening or closing and indicate what hardware and software were used.

Authors : Granulometric analysis by opening and closing is very similar to sieving. The size of sieve correspond to the size of the structuring element. During sieving the particles smaller than the sieve are eliminated. By opening the details smaller than the size of structuring element are also eliminated. In the sieving, the measure is the weight of the powder which does not eliminated. In image analysis the measure is the volume. The hardware and software used are cited in the text (Visilog software, Sun computer and image processor Imaging Technologies). But other systems can be used if the morphological operators are included in the package.